IMPROVED BOUNDARY CONDITIONS FOR ASSEMBLY-LEVEL TRANSPORT CODES

Kevin T. Clarno and Marvin L. Adams
Texas A&M University
Department of Nuclear Engineering, 3133 TAMU, 77843-3133
ktclarno@cedar.tamu.edu mladams@tamu.edu

ABSTRACT

We introduce and test a new methodology for including the effects of dissimilar neighbors on a given assembly's few-group parameters. Single-assembly calculations account for these effects through energy- and angle-dependent albedos; these are estimated from simple 1D transport solutions. A given albedo-condition calculation is a branch case, with the branching parameter being a change in a material concentration in a neighboring assembly. (The base case is, as usual, all identical neighbors.) The full effect of a different neighbor on a given assembly's parameters is approximated by superposition of the effects calculated in the branch cases. Results are very encouraging.

1. INTRODUCTION: THE INTERFACE PROBLEM

One of the main challenges that a reactor analysis methodology faces is obtaining the power distribution and averaged cross sections for an assembly whose neighboring assemblies are significantly different. If the neighbors are identical to the assembly in question, then an excellent approximation to the solution in the assembly can be obtained by solving a two-dimensional single-assembly problem with reflecting boundaries. However, if a neighboring assembly is significantly different, the reflecting boundary condition does not accurately model reality.

Reactor analysts have tried many different approaches to approximating the effects of unlike neighbors on an assembly's averaged cross sections. The most straightforward is to run multi-assembly calculations ("colorsets"), one for each four-assembly permutation that will appear in the core.[1,2] While straightforward in principle, this approach is computationally unwieldy and is taxing to the user. Thus, most analysis systems attempt to retain the single-assembly calculation and somehow account for the effects of different neighbors.

In this paper we describe a new methodology for capturing the effects of different neighbors by using the following detailed angle- and energy-dependent albedo boundary conditions:

$$\psi_g\left(\underline{r}_s,\underline{\Omega}\right)=\alpha_g\left(\underline{r}_s,\underline{\Omega}\right)\psi_g\left(\underline{r}_s,\underline{\Omega}'\right),\quad \underline{\Omega}'\equiv \text{ angle that reflects onto incident angle } \underline{\Omega}. \qquad (1)$$

Here ψ is angular flux and α is our specialized albedo. (A general albedo function relates each incoming $\left(g,\underline{\Omega}\right)$ to *all* outgoing $\left(g',\underline{\Omega}'\right)$.) While albedo boundary conditions have been explored before, our approach is different and offers several advantages. In the following section we set the stage by discussing general considerations and describe how our proposed methodology meshes with current methodology. In Section III we describe our calculation that produces the energy- and angle-dependent albedos that the single-assembly calculation is to use. In Section IV we discuss the cross sections that go into the calculation of these albedos. In Section V we discuss how the global-

reactor calculation will use the new information we create. We offer a summary and conclusions in the final section.

2. GENERAL CONSIDERATIONS

It is important to remember that current reactor-analysis methodology is reasonably accurate, even given single-assembly calculations with reflecting boundaries. Even on the most difficult commercial-reactor problems, the current methodology produces pin-power distributions that err by only a few percent.[3,4] This suggests that radical changes in the methodology are not needed; rather, we should carefully extend the existing methodology to try to capture most of the effect of different neighbors (and thus eliminate most of the error in today's calculations).

Current methodology employs single-assembly calculations to generate "base-case" few-group constants (cross sections, diffusion coefficients, and discontinuity factors), where "base-case" means a given set of parameters such as temperatures, power density, soluble boron or void concentration, etc. The variation of the constants with respect to changes in each parameter is estimated by solving one or more "branch cases" for each parameter. In a branch case on soluble boron concentration, for example, all other parameters are held at their base values, the boron concentration is changed, and the single-assembly calculation is performed. A branch on parameter p generates an estimate of dC/dp for each few-group constant C.

In addition to group constants, current methodology also generates a "form function." This function is the ratio of the power calculated by the reference method (fine-mesh many-group transport on heterogeneous assembly) to the power calculated by the global-analysis method (coarse-mesh few-group diffusion on homogenized assembly). This "function" is discretized as one number per pin cell. Its base-case value and its variation with respect to branch parameters, df/dp, is calculated and stored along with the group constants.

Our proposed methodology is a natural extension of this. We propose to add branch cases on parameters that describe the difference between the current assembly and its neighbors. Likely branch parameters would be fractional differences in fissile U content, Pu content, water content, and absorber content. Each branch case will be a single-assembly calculation with albedo boundary conditions on one surface, with the albedos chosen to represent a neighbor with the selected difference. The result will be the same type of dC/dp and df/dp values as are currently generated; there are simply additional p's to consider.

In a reactor, even an assembly that is surrounded by identical neighbors will not in general encounter mirror symmetry at any of its surfaces. Global "tilts" in the flux, caused for example by the finite size of the reactor, introduce non-zero currents at interfaces. We have developed a procedure to estimate this effect, building on our methodology for estimating the effects of different kinds of neighbors. The procedure uses a "tilt" branch case to estimate the change in form function and group constants as a function of global tilt.

3. ESTIMATING THE BRANCH-CASE ALBEDOS

Consider the following two-dimensional approximation of a real assembly (denoted "L" below) with an unlike neighbor (denoted "R") on one side:

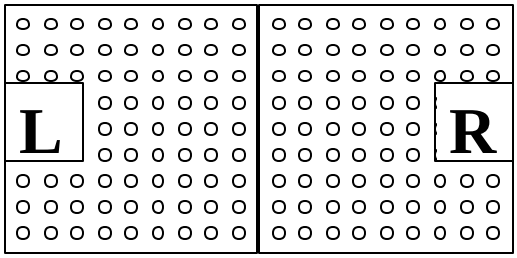

Figure 1. Interface between unlike assemblies.

If we knew exactly what materials were in region "R", we could solve a two-assembly transport problem to obtain the angular flux, y_g, at the interface. At that point we could define:

$$g_g\left(\underline{r}_s,\underline{\Omega}\right)=y_g\left(\underline{r}_s,\underline{\Omega}\right)/y_g\left(\underline{r}_s,\underline{\Omega}'\right). \qquad (2)$$

(If R were a mirror image of L, then g would equal 1 for each group and angle.) If this energy- and angle-dependent albedo were used as a boundary condition for assembly L, then a single-assembly solution in L would be identical to the two-assembly solution. We wish to avoid solving multi-assembly problems; thus, this definition at first appears to be of little value.

The effect of a "different" neighbor is fairly localized to a good approximation (because thermal neutron mean-free paths are very small compared to the assembly width); thus, much of the interface physics is effectively one-dimensional in space. Further, because g is a ratio of angular fluxes, it should be relatively insensitive to symmetric changes in geometric details. We therefore propose to estimate the albedo by solving a 1D problem with two homogeneous regions, as depicted in Fig. 2. Each region has the width of a half-assembly, and we employ reflecting boundaries on the outer edges.

This problem is simple enough that an accurate numerical solution will incur reasonable computational cost. We are using a linear-discontinuous finite-element method in space, multigroup in energy, and discrete-ordinates in angle, with logarithmically spaced spatial zoning at the interface, to quickly calculate the solution, which we then use to estimate the albedo:

$$g_g\left(\underline{r}_s,\underline{\Omega}\right)=g_g\left(\underline{r}_s,m,q\right)\approx y_g^{1\mathrm{DH}}\left(\underline{r}_s,m\right)/y_g^{1\mathrm{DH}}\left(\underline{r}_s,-m\right),\quad m=\mathrm{cosine}\left(\underline{\Omega}\bullet\underline{n}\right)<0. \qquad (3)$$

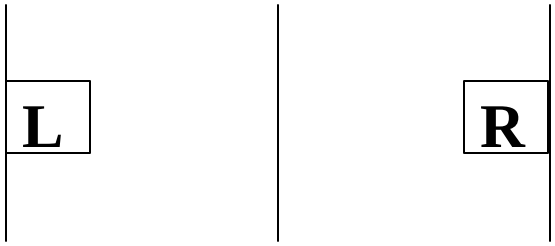

Figure 2. Approximate 1D model of interface between assemblies.

In Fig. 3 we present the estimated albedos from our 1D calculation at an interface between homogenized MOX and UO_2 assemblies. This figure shows the albedo for every fourth energy group of a 40-group set in which groups 1-11 are fast, 12-29 are epithermal, and 30-40 are thermal.

There is significant variation among the albedo functions for different groups in the fast energy range. The same is true for the epithermal and thermal ranges. Thus, an accurate representation of the interface physics will probably require albedos in the energy-group structure that is used for the single-assembly calculation – a coarser group structure is not likely to suffice. We therefore calculate our homogenized 1D albedos using the single-assembly group structure.

To estimate the effect of a global tilt, we plan to use material L in region R but change the boundary conditions on the outer edges to create a net flow of neutrons across the system. We plan to tabulate the resulting changes in form functions and group constants as functions along with the few-group ratios of net current to scalar flux at the internal interface.

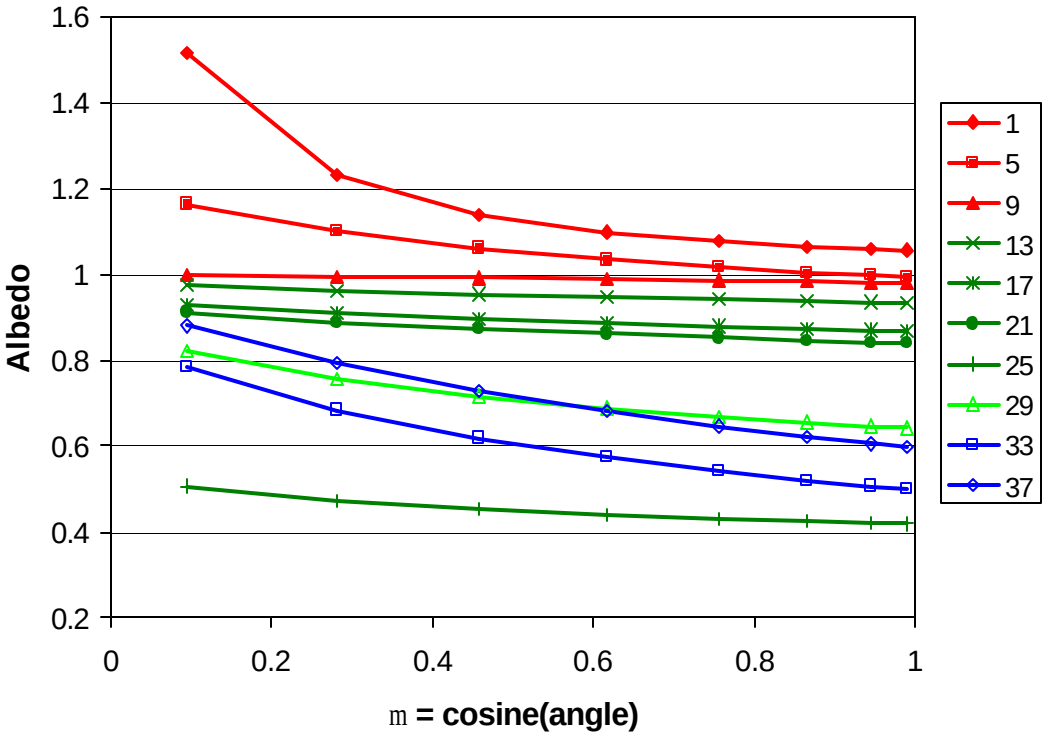

Figure 3. Albedo for every 4th energy group of a 40-group set.

4. HOMOGENIZED "NEIGHBOR" CROSS SECTIONS

The calculation of the albedo uses homogenized cross sections for an assembly that has a different concentration of some material. To produce these homogenized cross sections we shall employ a single-assembly calculation with reflecting boundaries. Thus, each of our "new" branch cases requires a single-assembly calculation (to generate homogenized neighbor cross sections), a 1D solution (to generate albedos), and another single-assembly calculation (which uses the albedos). We remark that the first single-assembly calculation will be less expensive than a typical single-assembly calculation – a relatively crude calculation will serve our purposes. Still, one "albedo" branch case will cost somewhat more than one "usual" branch case. We do not expect this to cause

significantly longer single-assembly run times, however, because we do not expect to add a significant number of branches relative to current practice.

5. RESULTS

The most difficult real-world commercial LWR problems involve LEU assemblies interspersed with MOX assemblies. We have considered several such problems to test our new methodology. We first explore the ability of the one-dimensional energy- and angle-dependent albedo to model the two-dimensional effects caused by neighboring assemblies. We then test the branch-case methodology of rebuilding group constants and form functions from branches on neighboring isotope concentrations, and finally test the complete methodology (which uses 1D albedos in branch-case calculations). All of our two-dimensional results were obtained with a modified version of TALC, a long-characteristics assembly-level transport code.[5,6] Each TALC calculation employed 8 flat-source regions in each pin cell, 7 energy groups, 4 polar angles, 4 azimuthal angles per quadrant, and 0.5-mm spacing between rays. Each assembly in our test problems was a uniform lattice of identical pin cells – there were no enrichment variations and no water holes. The circular pins were represented exactly.

5.1 ONE-DIMENSIONAL ALBEDO METHOD

Our goal is to tabulate information that allows us to accurately reproduce an assembly's few-group constants and form functions for any set of neighbors that the assembly can encounter. Figure 4 illustrates the three four-assembly test problems that we developed to test each step of our new methodology. We began by calculating each four-assembly test problem using TALC, thereby generating our reference results that we call "exact."

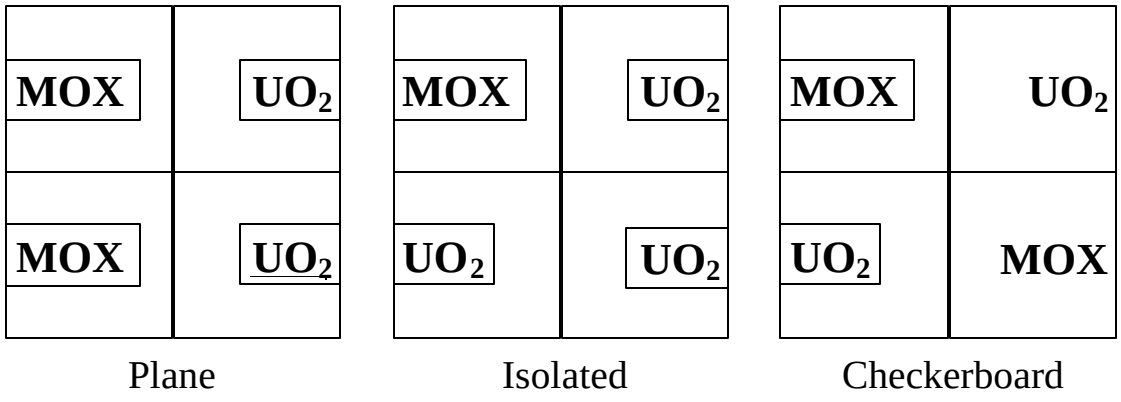

Figure 4. The three 2D test configurations.

Next, the top-left MOX assembly of each colorset was analyzed with various boundary conditions on the bottom and right edge of the assembly. For each colorset, a set of "true" energy- and angle-dependent albedos was calculated using exact angular fluxes that were spatially averaged over each pin-cell. Calculations using this set of albedos allow us to assess the importance of the spatial distribution of the albedo along each individual pin-cell edge. In addition, a reflective boundary condition was utilized to determine the errors that result from the "current" methodology. Using the known multi-group homogenized cross-sections of the neighboring UO_2 assembly, we calculated the "1DH" albedo from our 1D calculation of an interface between homogenized MOX and UO_2

assemblies. This albedo was used as the boundary condition at the MOX/UO_2 interfaces to calculate the "1DH" few-group parameters.

The plane configuration will test albedos calculated from a 1D homogenized problem on a 2D lattice that is uniform in one direction and thus has large-scale variations only in one dimension. As shown in the Table I, the new 1DH cross-sections have an order of magnitude smaller error than those of the current methodology. In addition, the eigenvalue (k-eff) used in the multi-group calculation also enjoys an order of magnitude improvement, which shows an improvement in the multi-group scalar flux spectrum that leads to the few-group cross sections. (This would increase in importance with additional energy groups in the multi-group calculation.) The error in the "true" calculations is caused only by spatial averaging over the pin-cell edges; it is very small. We conclude from this and other tests that the 1D homogenized albedos are exceptionally accurate for a 2D lattice that is uniform in one direction. This is a very encouraging result.

Table I. Results from the "Plane" test problem.

		Relative Error		
	Exact Value	**True**	**1DH**	**Current**
K-eff	**1.2329**	0.01%	0.28%	5.74%
Cross Sections				
Fast Group				
Total	**0.5527**	-2.5E-07	-0.04%	0.20%
Absorption	**0.0147**	-9.2E-06	-0.06%	0.59%
Nu-Fission	**0.0103**	0.005%	1.2E-06	0.22%
Fission	**0.0037**	0.005%	-0.002%	0.23%
to Fast	**0.5222**	-1.7E-06	-0.04%	0.16%
to Thermal	**0.0158**	0.006%	-0.12%	1.27%
Thermal Group				
Total	**1.6368**	-0.003%	-0.001%	0.20%
Absorption	**0.2413**	0.018%	0.04%	0.02%
Nu-Fission	**0.3848**	0.019%	0.04%	0.00%
Fission	**0.1372**	0.019%	0.04%	0.02%
to Fast	**0.0031**	0.002%	-0.02%	-1.35%
to Thermal	**1.3924**	-0.007%	-0.01%	0.24%
Avg. |C-S Error|		0.007%	0.03%	0.38%
K-inf (2-group)	**1.1624**	0.004%	0.01%	0.02%
Fast/Thermal Flux Ratio	**14.5382**	-0.005%	0.49%	-7.42%
Maximum Relative Pin Power Error		0.090%	0.99%	20.40%
Relative RMS Pin Power Error		0.007%	0.06%	1.30%
Jx/Phi (right edge)	**-0.00593**	-0.06%	5.8%	100.00%

Table II displays results from the isolated configuration. In this configuration, the actual albedo far from the four-assembly intersection is close to the 1D value, but it is closer to unity near the intersection. Therefore, the 1DH albedo is reasonably accurate away from the corners but is too large in the thermal groups near the corner, resulting in an over-estimated k-eff and a high corner pin

power. On the other hand, the reflective boundaries of the current methodology lead to an underestimate of the eigenvalue and a low corner pin power. Despite the strong corner effects of the problem, the 1DH method yields a factor of three reduction in average cross-section error and an order of magnitude reduction in error in the fast/thermal scalar flux ratio. However, the large maximum pin-power error (23.5%) indicates that the 1DH model needs improvement. We remark that the error in the "true" albedo calculation, whose only approximation is to use averages over each pin-cell edge, indicates that the albedo is sharply varying *spatially* along a single pin-cell edge; this is of course what happens near the point of intersection.

Table II also contains a column of results labeled "2D." These results were generated with a very simple modification of the 1DH albedos, which we shall describe in a later subsection.

Table II: Results from the Isolated configuration.

		Relative Error			
	Exact Value	**True**	**2D**	**1DH**	**Current**
K-eff	**1.2659**	0.04%	-1.8%	-3.3%	8.2%
Cross Sections					
Fast Group					
Total	**0.5531**	-0.001%	-0.19%	-0.22%	0.27%
Absorption	**0.0147**	-0.052%	-0.38%	-0.48%	0.83%
Nu-Fission	**0.0103**	-0.005%	-0.10%	-0.14%	0.31%
Fission	**0.0037**	-0.006%	-0.11%	-0.15%	0.33%
to Fast	**0.5224**	0.100%	-0.17%	-0.20%	0.20%
to Thermal	**0.0160**	0.477%	-0.52%	-0.74%	2.05%
Thermal Group					
Total	**1.6399**	0.03%	0.04%	-0.02%	0.40%
Absorption	**0.2407**	-0.25%	-0.21%	-0.20%	-0.25%
Nu-Fission	**0.3839**	-0.27%	-0.23%	-0.21%	-0.29%
Fission	**0.1369**	-0.27%	-0.22%	-0.22%	-0.26%
to Fast	**0.0031**	-0.26%	-0.10%	0.29%	-2.49%
to Thermal	**1.3961**	0.12%	0.08%	0.01%	0.52%
Avg. |C-S Error|		0.15%	0.20%	0.24%	0.68%
K-inf (2-group)	**1.1630**	0.02%	0.04%	0.04%	0.06%
Fast/Thermal Flux Ratio	**13.7022**	-0.31%	0.81%	2.7%	-14.0%
Maximum Relative Pin Power Error		0.60%	3.8%	23.5%	28.3%
Relative RMS Pin Power Error		0.02%	0.17%	0.65%	1.5%
Jx/Phi (right edge)	**-0.00393**	0.28%	-53%	100.00%	-36%

The checkerboard configuration is the most difficult of the three for the 1DH albedo. This problem has a saddle point at the four-assembly intersection where the net current goes to zero but the actual albedos are complicated. Relative to the reflecting-boundary calculation (labeled "current"), the 1DH albedo produces a more accurate fast/thermal flux ratio, a lower average cross-section error, and marginally lower root-mean square (RMS) error in pin power. However, the improvements are

marginal and not uniform, and would certainly not compel anyone to adopt the 1DH methodology over the current reflecting-boundary practice.

Table III: Results from the checkerboard configuration.

		Relative Error			
	Exact Value	**True**	**2D**	**1DH**	**Current**
K-eff	**1.2301**	0.04%	-4.8%	-6.3%	5.5%
Cross Sections					
Fast Group					
Total	**0.5524**	-0.001%	-0.30%	-0.34%	0.16%
Absorption	**0.0146**	-0.052%	-0.64%	-0.74%	0.57%
Nu-Fission	**0.0103**	-0.004%	-0.20%	-0.24%	0.21%
Fission	**0.0037**	-0.006%	-0.22%	-0.25%	0.22%
to Fast	**0.5219**	-4.8E-06	-0.27%	-0.30%	0.10%
to Thermal	**0.0159**	0.043%	-0.96%	-1.18%	1.62%
Thermal Group					
Total	**1.6394**	0.03%	0.00%	-0.06%	0.37%
Absorption	**0.2407**	-0.25%	-0.21%	-0.20%	-0.24%
Nu-Fission	**0.3839**	-0.27%	-0.22%	-0.21%	-0.29%
Fission	**0.1369**	-0.27%	-0.22%	-0.21%	-0.26%
to Fast	**0.0031**	-0.04%	0.12%	0.51%	-2.26%
to Thermal	**1.3955**	0.08%	0.04%	-0.03%	0.48%
Avg. |C-S Error|		0.09%	0.28%	0.36%	0.57%
K-inf (2-group)	**1.1632**	0.02%	0.06%	0.06%	0.07%
Fast/Thermal Flux Ratio	**13.8963**	-0.32%	2.2%	4.0%	-12.4%
Maximum Relative Pin Power Error		0.80%	8.3%	39.1%	19.2%
Relative RMS Pin Power Error		0.02%	0.4%	1.0%	1.3%
Jx/Phi (right edge)	**-0.00198**	0.53%	-169%	-203%	100.00%

5.2 A SIMPLE CORRECTION FOR THE 1DH ALBEDO

The corner effects of the isolated and checkerboard configurations cause the 1DH albedo to err significantly near the four-assembly interface. As shown in Tables II and III, this results in a very high maximum relative pin power error for the 1DH case, despite a reduced RMS error. To study the spatial shape of the albedo, we divide the albedos along the bottom of the assembly into "east" and "west" (with a corresponding "north" and "south" on the right edge), such that the east albedo is the angular flux in a northeast direction divided by its mirror angular flux in a southeast direction and the west albedo is the angular flux in a northwest direction divided by its mirror angular flux in the southwest direction:

$$g_g\left(\underline{r_s},\Omega_x,\Omega_y\right) \equiv \begin{Bmatrix} g_g^{east}\left(\underline{r_s},\Omega_x,\Omega_y\right), & \Omega_x > 0, \\ g_g^{west}\left(\underline{r_s},\Omega_x,\Omega_y\right), & \Omega_x < 0, \end{Bmatrix}, \quad \Omega_y > 0 \ . \tag{4}$$

In the southwest corner of the MOX quarter-assembly, near the reflective boundary, the 1DH albedo is nearly identical to the actual albedo of both the isolated and checkerboard configurations because it is far from the corner and therefore sees a nearly planar configuration. As we move closer to the corner, the angular flux contributing to the east albedo is coming from the bottom UO_2 assembly and is affected only indirectly by the lower-right assembly, through scattering and fission. Therefore, there is relatively little spatial variation of the east albedo along the bottom of the MOX assembly, as shown in Figure 5 (left graph), and thus it is reasonably well represented by the 1DH albedo. In contrast, the angular flux streaming from the lower-right assembly has a very direct effect on the west albedo near the corner, and thus we see more variation near the corner (right graph of Fig. 5).

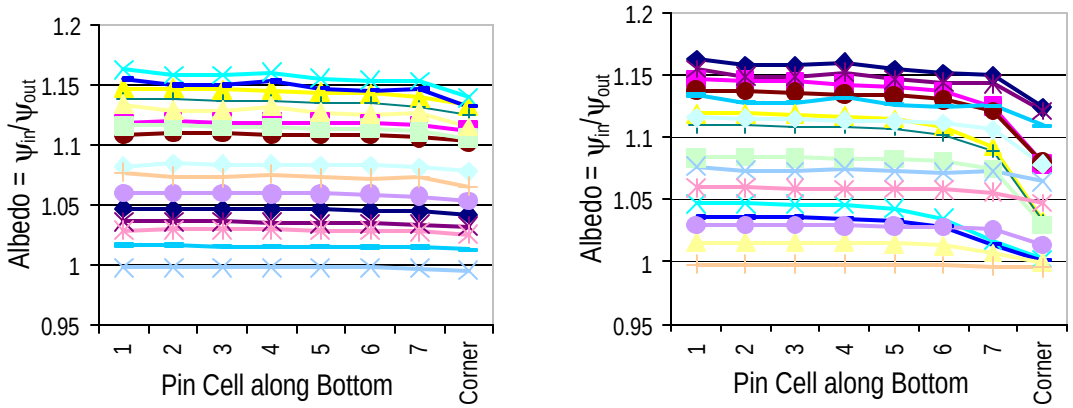

Figure 5. Actual albedos along bottom edge of MOX quarter-assembly, isolated configuration, group 4, 4 polar angles, 4 azimuthal directions per quadrant.
Left: actual "east" albedos. Right: actual "west" albedos.

Similar comments hold for the checkerboard configuration. In Figure 6 we see that the east albedos have less spatial variation than the west, and that both east and west are relatively flat close to the reflecting boundary (pin 1). As previously noted, there is a saddle point in the checkerboard configuration at the four-assembly intersection, at which the net current is zero. Although the angle-dependent albedos are not unity at this point, they are unity in an average sense (because the net current is zero). This character can be seen in Figure 6 (right graph).

These observations led us to try a very simple modification of the 1DH albedos, mainly to assess whether or not simple modifications could lead to significantly improved results. Because the 1DH albedo makes its largest error in west directions on the corner pin surface, we changed only the west albedo on the corner pin surface and retained 1DH for all other albedos. Our very simple modification is to simply set the west corner-pin albedo to unity. We do not offer this as a final solution; it is simply an experiment to see whether simple changes to 1DH can significantly improve its accuracy in problems with strong 2D character.

The results from this modified albedo, labeled "2D" in Tables II and III, suggest that this is the case. If we compare results from the current practice (reflecting), the 1DH albedo, and the 2D modification of the 1DH albedo, we can make the following observations. First, neither 1DH nor 2D produces dramatic improvements in few-group cross sections; however, errors in cross sections were already fairly small. Second, 1DH does significantly the fast/thermal flux ratio, and the 2D modification reduces the error by another factor of 2 or 3. Most importantly, the simple 2D

modification produces a dramatic improvement in spatial distribution. RMS pin-power errors are substantially reduced and the maximum pin-power error is reduced even further.

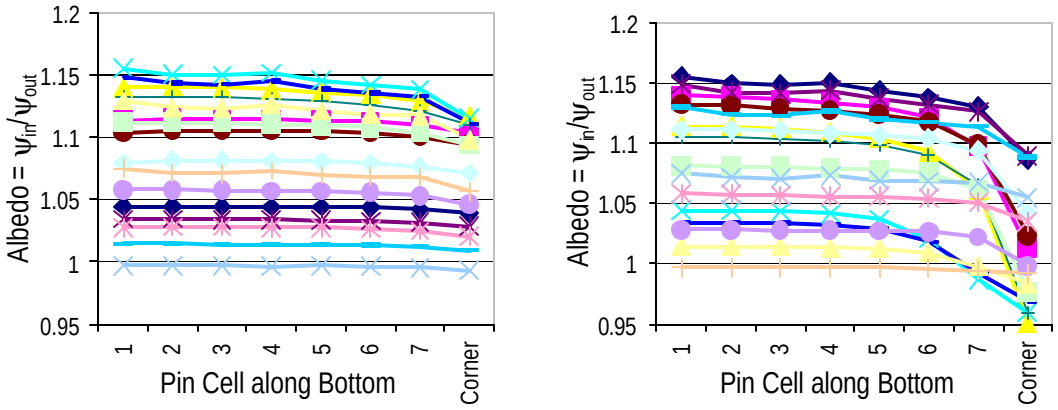

Figure 6. Actual albedos along bottom edge of MOX quarter-assembly, checkerboard configuration, group 4, 4 polar angles, 4 azimuthal directions per quadrant.
Left: actual "east" albedos. Right: actual "west" albedos.

We provide more detail about power distribution in Figures 7 (isolated) and 8 (checkerboard), in which pin powers are compared along the bottom row and along the diagonal of the MOX quarter-assembly. The reflecting-boundary calculation produces uniform pin powers of unity, which are not shown, but which are obviously quite different from reality. The 1DH albedo produces the correct trend of increasing power toward the corner, but it overshoots by quite a bit. The very simple modification to the west albedo on only the corner pin surface produces a significantly more accurate power distribution, with maximum error falling from 23% to 4% (isolated) and 39% to 8% (checkerboard).

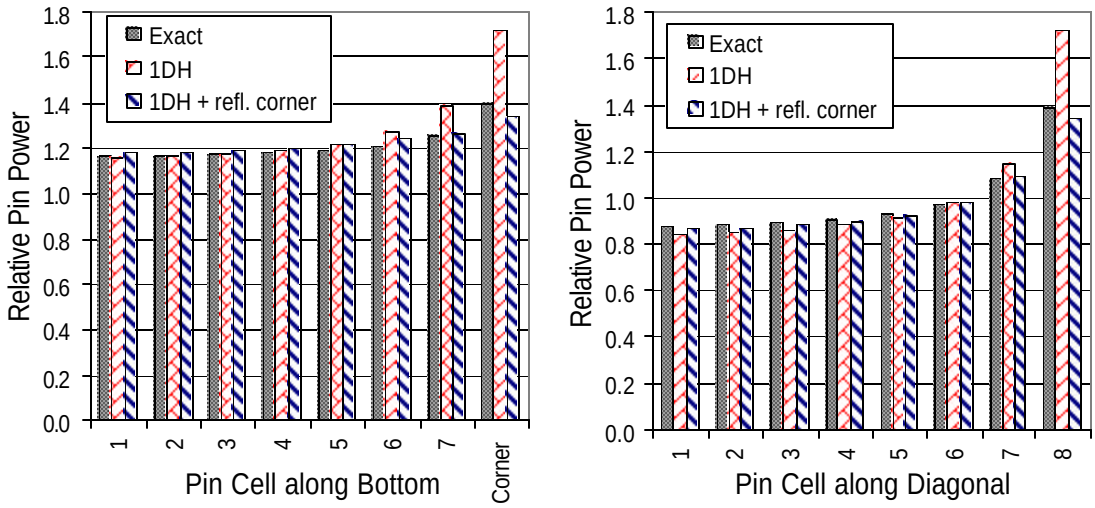

Figure 7. Pin powers in MOX assembly, isolated configuration, along bottom and diagonal. Simple model of unit albedos on corner pin surface reduces maximum error from 23% to 4%.

We reiterate that we are not proposing this simple, crude modification of the 1DH albedo as a practical algorithm for 2D calculations. The purpose of these results is only to show that simple modifications can produce significant improvements. Encouraged by these results, we are now working on a more systematic development of simple modifications to 1DH albedos for 2D problems.

These results of Tables I-III and Figures 5-8 suggest that we can accurately simulate the presence of unlike neighbors in a single-assembly calculation by using energy- and angle-dependent albedos generated from simple 1D calculations (with simple modifications for strongly 2D configurations). This is encouraging, but it is only one part of the machinery that we have proposed. Another key part is to use superposition of partial effects to build the full effect of a different neighbor, as implied by the branch-case methodology we described previously. We test this part of the methodology in the next subsection..

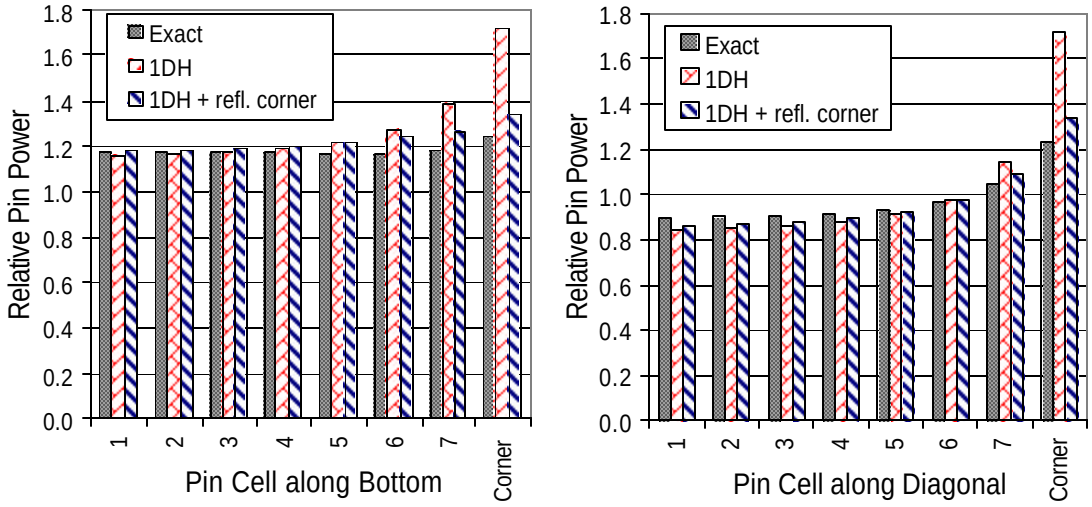

Figure 8. Pin powers in MOX assembly, checkerboard configuration, along bottom and diagonal. Simple model of unit albedos on corner pin surface reduces maximum error from 39% to 8%.

5.3 SUPERPOSITION METHOD USING THE 1DH ALBEDO

To analyze the superposition assumption of the new methodology we work with the plane-configuration model problem shown previously. Because the 1DH albedo produced very accurate results for this problem, it allows us to focus on errors generated only by the superposition approximation, not "contaminated" by errors induced by large-scale 2D features.

We are interested in the effect of a UO_2 neighbor on a MOX assembly. Our superposition approximation is that this is the sum of two independent effects: one caused by the neighbor having a different Pu concentration and one caused by it having a different U-235 enrichment. We first calculate the effect of a different Pu concentration, then the effect of a different U enrichment, and then combine those effects to estimate the effect of the neighbor (which of course has both a different Pu concentration and a different U enrichment).

Two new multi-group cross-section sets were calculated by modifying the isotopic makeup of the MOX assembly. One set had a increased enrichment of U-235 (2.88% instead of 1.44%); the

other had a reduced amount of total Pu (0.8% instead of 4.0%). Each set was used for the neighbor in a 1D homogenized calculation, which generated a 1DH albedo, which was used in a single-assembly calculation to produce few-group parameters. Partial derivatives of the MOX few-group cross-sections, form functions, and fast/thermal flux ratios were then determined with respect to the neighbor's U-235 and Pu fractions. These were then used to estimate the few-group parameters of the MOX assembly with a UO_2 (4.0% enriched) neighbor. The cross-section partial derivatives are presented in Table IV; the few-group parameters built from these partial derivatives are examined in Table V.

Table IV: Calculated Partial Derivatives of the Cross-Sections. ("Exact γ" results are from full colorset calculations, which are equivalent to as using an exact albedo instead of 1DH.)

	U-235		Total Pu	
	Exact	**1DH**	**Exact**	**1DH**
Fast Group				
Total	1.6E-04	1.4E-04	1.8E-04	5.9E-05
Absorption	3.9E-06	2.1E-06	2.4E-06	-3.1E-06
Nu-Fission	-2.1E-07	-7.1E-07	-4.2E-08	-1.1E-06
Fission	-1.2E-08	-2.0E-07	5.2E-08	-3.6E-07
to Fast	1.5E-04	1.4E-04	1.9E-04	8.1E-05
to Thermal	1.8E-08	-1.7E-06	-9.2E-06	-1.9E-05
Thermal Group				
Total	-3.1E-04	-3.3E-04	-1.3E-03	-1.4E-03
Absorption	4.5E-05	9.3E-06	2.3E-06	3.4E-05
Nu-Fission	8.1E-05	2.1E-05	2.4E-05	7.9E-05
Fission	2.7E-05	5.5E-06	5.5E-07	2.0E-05
to Fast	3.2E-06	3.6E-06	1.5E-05	1.6E-05
to Thermal	-3.6E-04	-3.4E-04	-1.3E-03	-1.4E-03

The first thing to note in Table IV is that many of the cross sections have very small partial derivatives. Examples include the fission, absorption, and upscattering cross sections. For some of these, the 1DH and exact albedos produce partial derivatives of different sign! This and similar discrepancies in Table IV are not significant because these derivatives are essentially zero, and they will therefore have little impact on the cross sections that are constructed later. For the larger cross sections, including total, the 1DH albedo produces partial derivatives that are quite close to those obtained from the exact colorset calculations.

In Table V we construct few-group MOX cross sections under the assumption of a UO_2 neighbor, using several different procedures. First, we perform the actual two-assembly problem with TALC and average the MOX cross sections to obtain the column labeled "Exact Value" in Table V. Second, we run with a reflecting boundary, which generates the usual un-corrected MOX cross sections. Third, we build cross sections from the partial derivatives shown in Table IV, once with derivatives obtained by colorsets and once with derivatives obtained using 1DH albedos. We compare relative errors in the last three columns of the table.

There is very little difference among the cross sections calculated with the reflecting boundary, the 1DH-albedo partial derivatives, and the exact partial derivatives. All cross sections have small errors – less than 1% except for the downscattering cross section. However, the fast/thermal flux ratio generated from the partial derivatives as well as the form function, are substantially more

accurate than those of the reflecting-boundary calculation. The error in fast/thermal ratio is reduced by approximately an order of magnitude, as is maximum pin-power error. We conclude that the new methodology significantly reduces the largest reflecting-boundary errors, but does not necessarily reduce errors that are already small.

Table V: Relative Error of the Calculated Cross-Sections from Superposition.

		Relative Error		
	Exact Value	**Reflecting**	**Exact g**	**1DH**
K-eff	1.1635	5.7%	5.6%	5.3%
Cross Sections				
Fast Group				
Total	0.5513	0.20%	0.26%	0.18%
Absorption	0.0146	0.59%	0.59%	0.47%
Nu-Fission	0.0102	0.22%	0.23%	0.20%
Fission	0.0037	0.23%	0.24%	0.21%
to Fast	0.5210	0.16%	0.23%	0.15%
to Thermal	0.0157	1.27%	1.03%	0.81%
Thermal Group				
Total	1.6378	0.20%	-0.06%	-0.08%
Absorption	0.2413	0.02%	-0.03%	0.06%
Nu-Fission	0.3849	0.00%	-0.03%	0.07%
Fission	0.1373	0.02%	-0.03%	0.07%
to Fast	0.0031	-1.35%	0.35%	0.42%
to Thermal	1.3934	0.24%	-0.07%	-0.11%
K-inf (2-Group)	1.1626	0.015%	-0.020%	-0.008%
Avg. |C-S Error|		0.38%	0.26%	0.24%
Fast/Thermal Flux Ratio	14.5382	-7.4%	-1.2%	-0.4%
Maximum Relative Pin Power Error		20.4%	4.4%	2.7%
Relative L-2 Pin Power Error		1.3%	0.4%	0.3%
Jx/Phi (right edge)	-0.0059	100%	162%	165%

6. GLOBAL CALCULATION

The global calculation in modern reactor analysis is performed using few-group coarse-mesh diffusion theory with homogenized assemblies. The few-group constants for each assembly are interpolated from tables generated by single-assembly transport calculations, as described previously. Our methodology does not change this, but simply adds to the interpolation space. We assume that the global code has access to enough information about neighboring assemblies that it can obtain the interpolation parameters (such as fractional difference in Pu content or U-235 enrichment) for each neighbor. It is then a simple matter to compute and sum (superimpose) the changes in few-group parameters that are induced by each material difference in each neighbor.

If global tilts are found to induce significant changes in cross sections or form functions, we can employ a strategy to account for them, as we now describe. In addition to partial derivatives of few-group parameters, the assembly-level calculations can tabulate the interface fast-group J/f ratio that is induced by each albedo-branch's perturbation. As few-group parameters are built during the global calculation, these J/f ratios can be summed to produce an estimate of the J/f that the global code "should" expect to see at each interface because of the different composition of the neighboring assemblies. This estimated J/f estimated can be subtracted from the actual J/f seen by the global code, and the difference, $\Delta(J/f)$, can be attributed to a global tilt. In a previous section we described a procedure for performing branch calculations with non-zero tilts; each such branch calculation can tabulate the fast-group J/f ratio at the interface along with the changes that are induced in the few-group parameters. The global code can then estimate the cross-section change induced by the global tilt, under the assumption that such a change is proportional to the J/f associated with that tilt.

7. SUMMARY AND CONCLUSIONS

We have developed an extension of present-day reactor-analysis methodology that systematically accounts for the effects that different neighbors have on a given assembly's few-group constants. The new technique centers on energy- and angle-dependent albedos that simulate the effect of the unlike neighbors. Each set of albedos defines a branch case and thus fits into the framework of present-day methodology. The parameter varied in each new branch case is the fractional difference in the neighbor's concentration of an isotope or mixture. (The base case corresponds to a zero difference in all concentrations – an identical neighbor – which produces the usual reflecting boundary condition.) The key simplification is that the albedos are generated by a one-dimensional transport calculation with a homogenized assembly and homogenized neighbor.

We have found that the albedo produced from 1D homogenized (1DH) calculations does an extremely good job of capturing the effects of different neighbors in the rather restricted case of lattices that are uniform in one direction (in which the only large-scale variation is in the other direction). In fully 2D problems, the 1DH albedos are accurate near the center of an interface but in general lose accuracy at corners. This loss of accuracy in the albedo produces large errors in corner-pin powers in the worst cases. We have found that very simple modifications to the 1DH albedos can dramatically reduce these large errors. This encouraging result has led us to pursue systematic (but simple) modifications that are theoretically sound and that produce very accurate results. We believe that this goal is attainable.

Our complete methodology relies on albedos to estimate the changes in few-group parameters that are induced by differences in a neighboring assembly's composition. Another part of the methodology is to assume superposition and thus build the change in a parameter by summing the partial changes from a variety of differences in a neighbor's composition. In our limited tests to date, we have found that the success of this superposition approach is mixed. Given a cross section that is not affected much by a different neighbor, the superposition methodology correctly finds a small change, but this does not necessarily make the cross section more accurate. Given a parameter that is significantly affected by a different neighbor, such as fast/thermal flux ratio or pin-power distribution, the superposition methodology appears to work quite well.

In summary, we believe the new methodology is promising, and we expect to continue to refine it, couple it to other pieces of a full reactor-analysis system, and test the coupled system. We hope to report on our progress in future communications.

ACKNOWLEDGEMENTS

We thank Dmitriy Anistratov, Todd Palmer, and Kord Smith for many helpful discussions. This work was supported by Nuclear Energy Research Initiative (NERI) Program of the US Department of Energy under grant No. DE-FG03-99SF21922.

REFERENCES

1. D. Knott et al., "CASMO-4 Methodology Manual," STUDSVIK/SOA-95/02, Studsvik of America (1995).
2. K. Smith, "MOX Analysis Methods in SIMULATE-3," *Trans. Am. Nucl. Soc.*, **76**, 181 (1997).
3. K. Rempe, K. Smith, "Mixed-Oxide and BWR Pin Power Reconstruction in SIMULATE-3," *PHYSOR 90*, Marseille, France, April 1990, Vol. 2, p. VIII-11.
4. S. Palmtag, A. Henry, "Advanced Nodal Methods for MOX Fuel Analysis," Massachusetts Institute of Technology, Nuclear Engineering Department, Ph.D. Thesis, September 1997.
5. M. R. Zika, "Iterative Acceleration for Two-Dimensional Long Characteristics Transport Problems," Texas A&M University, Department of Nuclear Engineering, PhD dissertation (M. L. Adams, advisor) (1997).
6. M. R. Zika and M. L. Adams, "Transport Synthetic Acceleration for Long-Characteristics Assembly-Level Transport Problems," *Nucl. Sci. Eng.*, **134**, 135-158 (2000).